

# Heavy Thallium Based Fluoroperovskite TIAF<sub>3</sub> (A = Ge, Sn and Pb) Compounds: A Computational Investigation

**Shams U Zaman**

Kohat University of Science and Technology

**Nasir Mehmood**

Kohat University of Science and Technology

**Sajid Khan**

Kohat University of Science and Technology

**Rashid Ahmad** (✉ [rashidahmad@kust.edu.pk](mailto:rashidahmad@kust.edu.pk))

Kohat University of Science and Technology <https://orcid.org/0000-0001-5945-0549>

**Nadia Sultan**

Kohat University of Science and Technology

**Farhat Ullah**

Kohat University of Science and Technology

**Altaf Ur Rahman**

Riphah International University - Lahore Campus

**H. J. Kim**

Kyungpook National University

---

## Research Article

**Keywords:** DFT, WIEN2k, GGA+U, Elastic properties, stable system

**Posted Date:** August 23rd, 2021

**DOI:** <https://doi.org/10.21203/rs.3.rs-740235/v1>

**License:**  This work is licensed under a Creative Commons Attribution 4.0 International License.

[Read Full License](#)

---

# **Heavy Thallium based Fluoroperovskite $\text{TIAF}_3$ , ( $\text{A} = \text{Ge, Sn and Pb}$ ) Compounds: A Computational Investigation**

Shams U Zaman<sup>a</sup>, Nasir Mehmood<sup>a</sup>, Sajid Khan<sup>a</sup>, Rashid Ahmad<sup>a\*</sup>, Nadia Sultan<sup>a</sup>, Farhat Ullah<sup>a</sup>, Altaf Ur Rahman<sup>c</sup>, H. J. Kim<sup>b</sup>

<sup>a</sup>Department of Physics, Kohat University of Science and Technology, Kohat, 26000, Khyber Pakhtunkhwa, Pakistan

<sup>a</sup>Department of Physics, Riphah International University Lahore Campus

<sup>b</sup>Department of Physics, Kyungpook National University, Daegu, 41566, South Korea

## **Abstract**

Combination of heavy elements in forming a stable system leads to enhancement in effective atomic number making it desirable in many applications such as detection and shielding of radiation. We present our theoretical investigations on new Thallium based heavy fluoroperovskites  $\text{TIAF}_3$  ( $\text{A} = \text{Ge, Sn and Pb}$ ). The study is carried out to explore the structural, elastic, electronic, and optical properties through the Density Functional Theory (DFT) using the Full-Potential Linearized Augmented Plane Wave (FP-LAPW) method implemented in WIEN2k. Generalized Gradient Approximation with consideration of electronic correlation effects (GGA+U) was employed for calculations. The lattice constants deduced from the optimization curves were found to be in the range of 4.00 Å to 4.85 Å. Elastic properties were obtained from the calculated elastic constants. From band structure calculations, it is evident that the bandgaps range from 0.84 to 1.89 eV. All the studied compounds exhibit indirect bandgap nature. Fluorine atom contributes significant number of electronic states in valence and conduction bands of all studied compounds. The optical response in terms of refractive index, extinction coefficient, optical conductivity, reflectivity, and absorption coefficients are calculated and discussed in the energy range of (0-20) eV. The properties of compounds in this study are being reported for the first time.

## **1. Introduction**

Perovskites are the class of materials having a simple structure of the form  $\text{ABX}_3$  and having potential applications owing to their diverse properties. Fluoroperovskites are the subclass of perovskites where X is replaced by Fluorine. Growing interest is being witnessed in the investigation of Flouropervoskites due to their properties such as ferroelectricity [1], as lens [2], phosphors [3], dosimeters [4], etc.

Density Functional Theory (DFT) can be employed to screen and design future materials. It can also serve to get an insight into the physical properties of interest. Fluoroperovskite systems composed of various elements are being actively investigated using DFT.

A comprehensive study was reported by S. Korbel et al. [5] on the search of thermodynamically stable cubic perovskites through high-throughput density functional theory calculations. In this study, the prediction of new stable perovskite systems opened up the way for a detailed investigation of physical properties. The versatile bandgap of perovskites ranging from semiconductors to insulators and the presence of a variety of elements in stable structures makes them worthwhile to investigate for various applications. We reported the study on Thallium-based fluoroperovskites  $TlXF_3$  ( $X = Ca, Cd, Hg$  and  $Mg$ ) [6] and predicted their use as scintillation material due to high effective atomic number and bandgap in the insulating region. In another study, the  $InAF_3$  ( $A = Ca, Cd$  and  $Hg$ ) system [7] was investigated by replacing Thallium with Indium, making materials more environment friendly owing to less toxicity of Indium.

The presence of heavy elements in a compound increases the effective atomic number ( $Z_{eff}$ ). The large value of  $Z_{eff}$  of a material makes it attractive for numerous applications such as radiation detection and radiation shielding. Incorporation of heavy elements in compounds like  $Bi_4Ge_3O_{12}$  [8],  $(Lu,Gd)_3(Ga,Al)_5O_{12}$  [9],  $Tl_2LiGdCl_6$  [10], and  $PbWO_4$  [11] makes materials promising for scintillation applications. Despite intensive research on fluoroperovskite systems, to the best of our knowledge, no study is performed on a combination of heavy elements with Thallium  $TlAF_3$  ( $A = Ge, Sn$  and  $Pb$ ). Therefore, we found it valuable to choose this system for exploring the structural, electronic, and optical properties using DFT with the WIEN2k package and predict properties for future experiments.

## 2. Methodology

The ternary compounds  $TlAF_3$  ( $X = Ge, Sn$  and  $Pb$ ) crystallize in the cubic perovskite-type crystal structure having space group  $Pm\bar{3}m$  (# 221). The Tl and A atoms are positioned at (0,0,0) and (1/2,1/2,1/2), respectively, while F atoms are placed at (0,1/2,1/2), (1/2,0,1/2) and (1/2,1/2,0) sites of the Wyckoff coordinates as shown in Fig.1.

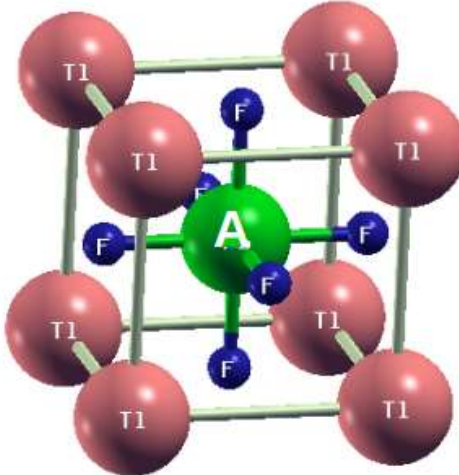


**Fig.1.** The unit cell structure of  $\text{TlAF}_3$  ( $\text{A} = \text{Ge}, \text{Sn}$  and  $\text{Pb}$ )

In this work, we have applied the full-potential linearized augmented plane wave method (FP-LAPW) [12] as implemented in WIEN2k [13] code to examine the different properties of compounds under consideration. The contribution of Coulomb interactions is included and calculations are carried out using generalized gradient approximation with additional Hubbard-U term for taking on-site Coulomb interaction (GGA+U) [14]. Structural optimization and the investigation of structural parameters are carried out by fitting energy versus volume using Burch Murnaghan's equation of state [15]. The energy difference between the core and valence states is taken to be -6 Ry. The spherical harmonic functions are used with the cut-off  $l\text{-max} = 10$  inside the muffin tin-spheres. Moreover, the RMT values for Tl is 2.5 for all compounds. In the case of  $\text{TlGeF}_3$ , 2.15, 2.11 for Ge, F, and in  $\text{TlPbF}_3$ , 2.11 is selected for both Pb and F. While in  $\text{TlSnF}_3$ , 2.12 is taken for both Sn and F atoms. The K Points are chosen to be 1500 and the G-max value is selected to be 12.

### 3. Results and Discussion

This section is dedicated to description and explanation of our calculated results for structural, elastic, electronic and optical properties of  $\text{TlAF}_3$  ( $\text{X} = \text{Ge}, \text{Sn}$  and  $\text{Pb}$ ) compounds.

#### 3.1. Structural and Elastic Properties

We performed volume optimization calculations on the unit cell of  $\text{TlAF}_3$  ( $\text{X} = \text{Ge}, \text{Sn}$  and  $\text{Pb}$ ). Such calculations gave the structural parameters of the compound such as the lattice constant ( $a_0$ ), bulk modulus (B), and pressure derivative of bulk modulus ( $B'$ ). The unit cell volume is varied,

and the corresponding total energy of the cell is calculated. The variation behavior is fitted by the Birch–Murangan equation of state as shown in Fig. 2. The volume at which energy became minimum is known as the ground state volume ( $V_0$ ). Corresponding to that volume, the ground state parameters  $a_0$  (Å),  $B$  (GPa), and  $B'$  are evaluated and presented in Table I.

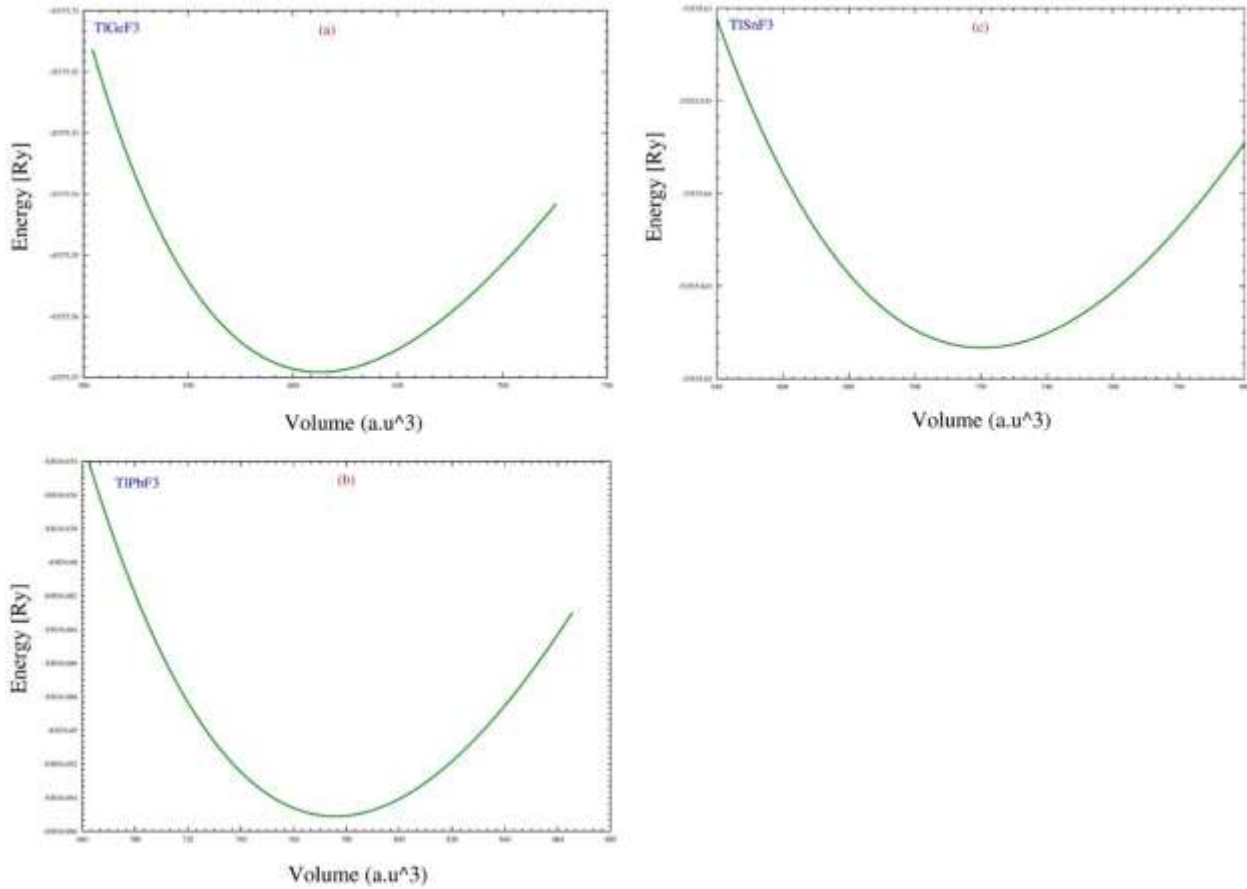


**Fig.2.** Volume optimization plots of Tl-based cubic perovskites  $\text{TlAF}_3$  ( $X = \text{Ge}, \text{Sn}$  and  $\text{Pb}$ ) by GGA+U method.

The mechanical properties of materials can be studied by employing the elastic constants  $C_{ij}$ . These constants are used to describe the response to macroscopic stress applied. They also provide a link between the mechanical and dynamic behavior of crystals and determine how the material is subjected to stress deformation and its recovery after the removal of applied stresses. The structural stability, bonding character between adjacent atomic planes, and anisotropic character can also be deduced from these constants. There are three distinct elastic constants of concern  $C_{11}$ ,  $C_{12}$ , and

$C_{44}$  for a cubic system. The calculated elastic constants  $C_{ij}$  are listed in Table I are positive and follow the conditions of mechanical stability [16]

$$C_{11} > 0; C_{44} > 0; (C_{11} - C_{12}) > 0;$$

$$(C_{11} + 2C_{12}) > 0; C_{12} < B < C_{11}.$$

Bulk Modulus (B), anisotropy factor (A), Young's modulus (E), Poisson's ratio (v) and Pugh's index ratio (B/G) found by using the below mathematical relations [17] are listed in Table I.

$$B = \frac{C_{11} + 2C_{12}}{3} \quad (1)$$

$$A = \frac{2C_{44}}{C_{11} - C_{12}} \quad (2)$$

$$E = \frac{9BG}{3B + G} \quad (3)$$

$$v = \frac{3B - 2G}{2(2B + G)} \quad (4)$$

$$G = \frac{G_v + G_R}{2} \quad (5)$$

$$G_v = \frac{C_{11} - C_{12} + 3C_{44}}{5} \quad (6)$$

$$G_R = \frac{5C_{44}(C_{11} - C_{12})}{4C_{44} + 3(C_{11} - C_{12})}. \quad (7)$$

The ductility and brittleness nature are studied by using the bulk modulus to shear modulus ratio (B/G) and Poisson's ratio (v). For under-study compounds, according to Pugh's ratio [18], values of B/G exceed the limit of 1.75 which is considered as its threshold value. While according to the Poisson ratio [19], calculated values of v for all compounds are greater than 0.26, so all the compounds are ductile in nature. The degree of elastic anisotropy of a crystal can be inferred from the anisotropy factor (A). If the value of A approaches unity, the crystal reveals isotropic character. The calculated values of A for all compounds are deviating from 1 as listed in Table II, so we can conclude that the compounds under consideration in this work are anisotropic mechanically.

**Table I.** The values of equilibrium lattice constants  $a_0$  (in Å), the three elastic constants  $C_{11}$ ,  $C_{12}$ ,  $C_{44}$  (in GPa), the values of anisotropy factor A, Bulk modulus B (in GPa), the shear modulus G (in GPa), Young's modulus E (in GPa), Poisson's ratio v and Pugh's index ratio B/G for  $\text{TIAF}_3$  ( $X = \text{Ge, Sn and Pb}$ ) by GGA+U method.

Parameter	$\text{TI}\text{GeF}_3$	$\text{TI}\text{SnF}_3$	$\text{TI}\text{PbF}_3$
$a_0$	4.49	4.00	4.85
$C_{11}$	163.40	442.52	274.55
$C_{12}$	60.46	147.22	112.47
$C_{44}$	36.03	62.96	63.53
A	0.70	0.57	0.78
B	94.77	245.65	166.50
G	41.57	105.67	70.03
E	108.81	277.26	184.27
v	0.43	0.44	0.44
B/G	2.27	2.32	2.37

### 3.2. Electronic Properties

This section presents the electronic properties of  $\text{TIAF}_3$  ( $A = \text{Ge, Sn and Pb}$ ). Band structure and density of states provides the information about the electronic behavior of a compound. The calculations, like for all other properties, are performed using GGA+U approach. Investigation of the structure of the energy band is very useful for understanding the electronic and optical properties of a material. Therefore, the calculated energy band structures of  $\text{TIAF}_3$  ( $A = \text{Ge, Sn and Pb}$ ) are obtained and demonstrated in Fig. 3. The states are plotted in the energy range of -6 to +6 eV, along with high symmetry directions in the first Brillouin zone (BZ). The horizontal dashed line represents Fermi level, set at zero energy level, and is indicated by a horizontal dashed line. The high symmetry points of irreducible BZ are marked with alphabetic letters. The position of valence band maxima and conduction band minima provides information about the bandgap nature. If both lie at the same symmetry point, then material is known to have direct band gap, otherwise the band gap nature is indirect. Fig. 3 shows that  $\text{TI}\text{GeF}_3$  with a bandgap of 1.67 eV is an indirect bandgap compound as its maxima of valence band positioned at R symmetry point and conduction band minima lie at M symmetry point.  $\text{TI}\text{SnF}_3$  also exhibits indirect bandgap nature at R-M symmetry points with a bandgap of 0.84 eV and  $\text{TI}\text{PbF}_3$  has a bandgap value of 1.89 eV showing indirect band behavior at R-M symmetry point. All the calculated values of bandgap at different symmetry points are listed in Table II.

To examine the thorough insight of the electronic structure of band gap, the elemental contribution for  $\text{TIAF}_3$  ( $A = \text{Ge, Sn and Pb}$ ) is evaluated as shown in Fig.4. In the case of  $\text{TI}\text{GeF}_3$ , shown in part (a), it is clear that in the valence region, maximum states are contributed by F atom in which among all of its orbitals, p-state has a major share. Whereas the conduction band has mixed contributions from Ge and F atoms. Part (b) of Fig.4 presents the total and partial density of states of  $\text{TI}\text{SnF}_3$ . It is obvious that the valence region is dominated by the states of F atom, especially p-state of the F atom. Sn atom also has some share of its states at the upper portion of the valence band. In the conduction band, there is mixed contribution from F and Sn atoms. On the other hand, in the case of  $\text{TI}\text{PbF}_3$ , the valence region is

dominated by the states of F atom while the conduction band is having mixed behavior contributed by F atom and p-states of Tl atom as shown in Fig. 4(c).

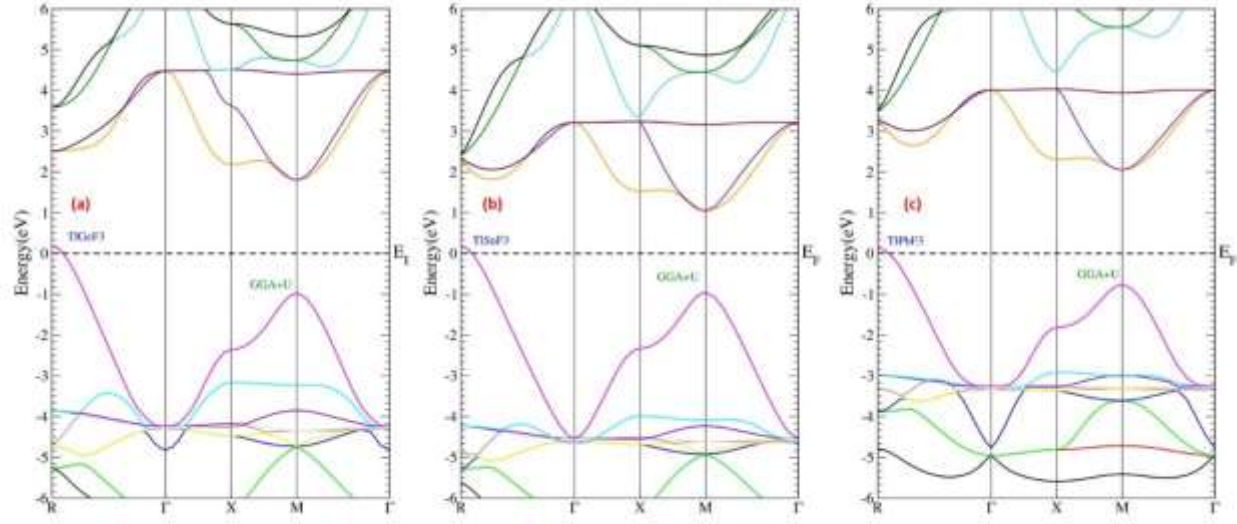


**Fig.3.** The calculated band structure of  $\text{TlAF}_3$  ( $\text{A} = \text{Ge}, \text{Sn}$  and  $\text{Pb}$ ) in high symmetry directions using GGA+U.

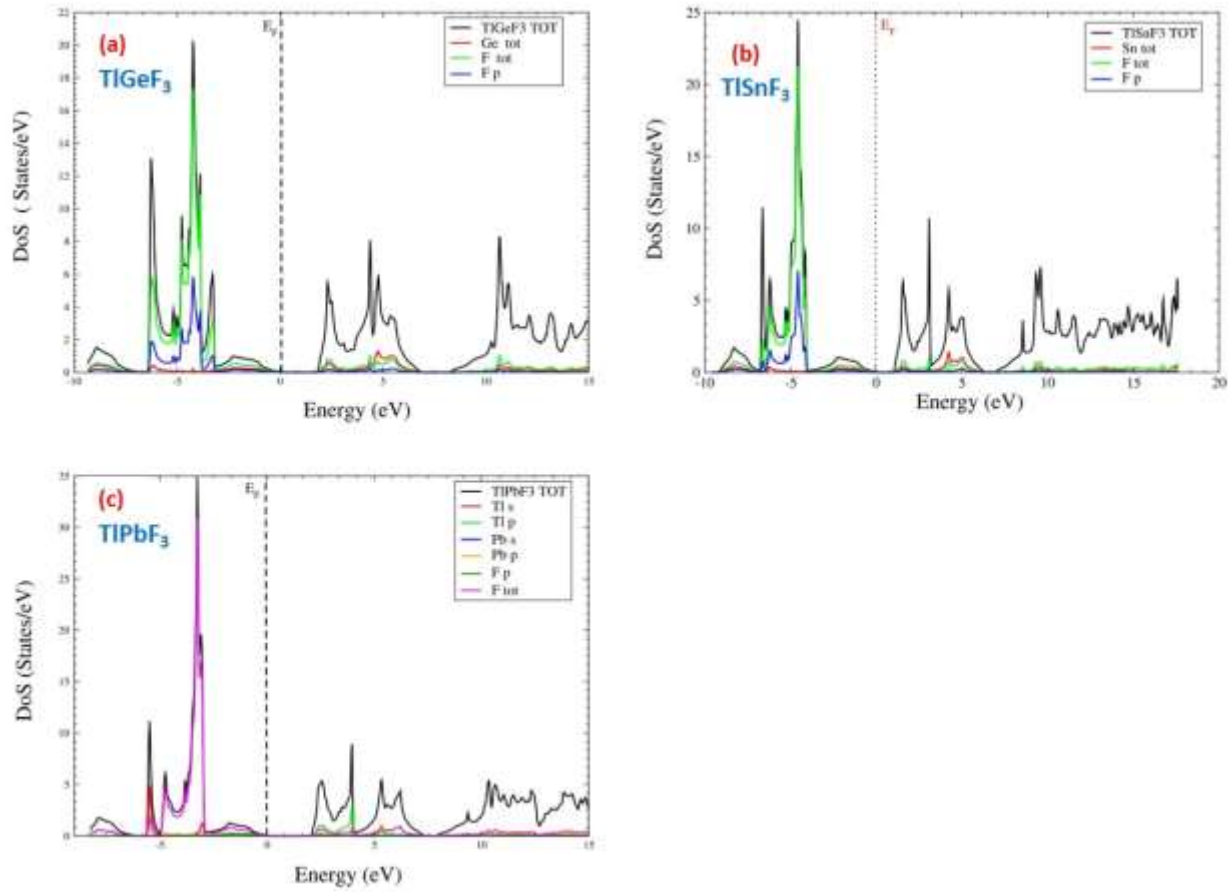


**Fig.4.** Total and partial density of states (TDOS and PDOS) of  $\text{TlAF}_3$  ( $\text{A} = \text{Ge}, \text{Sn}$  and  $\text{Pb}$ ) compounds (GGA+U).

**Table II.** Bandgap values of  $\text{TlAF}_3$  ( $\text{A} = \text{Ge}, \text{Sn}$  and  $\text{Pb}$ ) were obtained through GGA+U.

Compound	$E_g^{M-M}$	$E_g^{X-X}$	$E_g^{F-F}$	$E_g^{R-M}$	$E_g^{R-X}$
<b>TlGeF<sub>3</sub></b>	2.83	4.49	8.74	1.67	6.40
<b>TlSnF<sub>3</sub></b>	1.95	3.83	7.66	0.84	6.00
<b>TlPbF<sub>3</sub></b>	2.75	4.10	7.24	1.89	5.52

### 3.3. Optical Properties

The optical behavior of  $\text{TlAF}_3$  ( $\text{A} = \text{Ge}, \text{Sn}$  and  $\text{Pb}$ ) compounds to incident photons having energies (0-20 eV) has been discussed in this section using GGA+U approach. All the calculated optical properties are plotted in Fig. 5. The complex dielectric function  $\epsilon(\omega)$  given by the

Ehrenreich and Cohen's equation has been used to explain these optical properties [20] and is given as:

$$\boldsymbol{\varepsilon}(\omega) = \boldsymbol{\varepsilon}_1(\omega) + i\boldsymbol{\varepsilon}_2(\omega). \quad (8)$$

The linear response of any medium to external electric and magnetic fields is calculated by this complex function.

The electronic band structure of a solid helps in the calculation of the imaginary part of dielectric function by using the following relation:

$$\boldsymbol{\varepsilon}_2(\omega) = \frac{4\pi^2 e^2}{m^2 \omega^2} \sum_{i,j} \int_k \langle i | \mathbf{M} | j \rangle^2 f_i(1 - f_j) \times \delta(E_{j,k} - E_{i,k} - \omega) d^3k. \quad (9)$$

Both initial and final states are represented by  $i$  and  $j$  respectively, while  $\mathbf{M}$  represents the dipole matrix. Similarly,  $f_i$  is the Fermi distribution function for the  $i^{\text{th}}$  state while electron energy in the  $i^{\text{th}}$  state is given by  $E_i$ .

The real part of dielectric function is found by using the Kramers-Kroning relation, given as:

$$\boldsymbol{\varepsilon}_1(\omega) = \mathbf{1} + \frac{2}{\pi} \mathbf{P} \int_0^\infty \frac{\omega' \boldsymbol{\varepsilon}_2(\omega')}{\omega'^2 - \omega^2} d\omega'. \quad (10)$$

Here  $\mathbf{P}$  represents the principal part of the integral in the above equation

The imaginary part of the dielectric function is related with the absorption behavior of a solid which is directly linked to electronic band structure. This part describes the electronic transitions occurring between the valence and conduction bands. Both real and imaginary parts play a vital role in obtaining the refractive index, extinction coefficient, absorption coefficient, and reflectivity.

The real part of the dielectric function  $\boldsymbol{\varepsilon}_1(\omega)$  is shown in Fig. 5(a), (h), and (o). The static dielectric constants  $\boldsymbol{\varepsilon}_1(0)$  for  $\text{TlGeF}_3$ ,  $\text{TlSnF}_3$ , and  $\text{TlPbF}_3$  are 4.1, 18.5, and 3.4, respectively. The imaginary part  $\boldsymbol{\varepsilon}_2(\omega)$  describing the absorption behavior of all compounds as a function of photon energies have been shown in Fig. 5(b), (i), and (p). The absorption edges of a compound have relation with energy bandgap. As we can see from the band structure plot,  $\text{TlSnF}_3$  has the smallest band gap among all compounds under study, therefore its absorption edge is located at the lowest photon energy among all compounds.

After that, the next edges are found for  $\text{TlGeF}_3$  and  $\text{TlPbF}_3$ , in the order of increasing band gaps in accordance with the band structure plot in Fig. 3. Beyond absorption edges, curves rapidly rise due to an increase in the number of states which contribute towards absorption. The major peaks are observed at energies of 7.6 eV, 0.7 eV, and 5.7 eV for  $\text{TlGeF}_3$ ,  $\text{TlSnF}_3$ , and  $\text{TlPbF}_3$ , respectively.

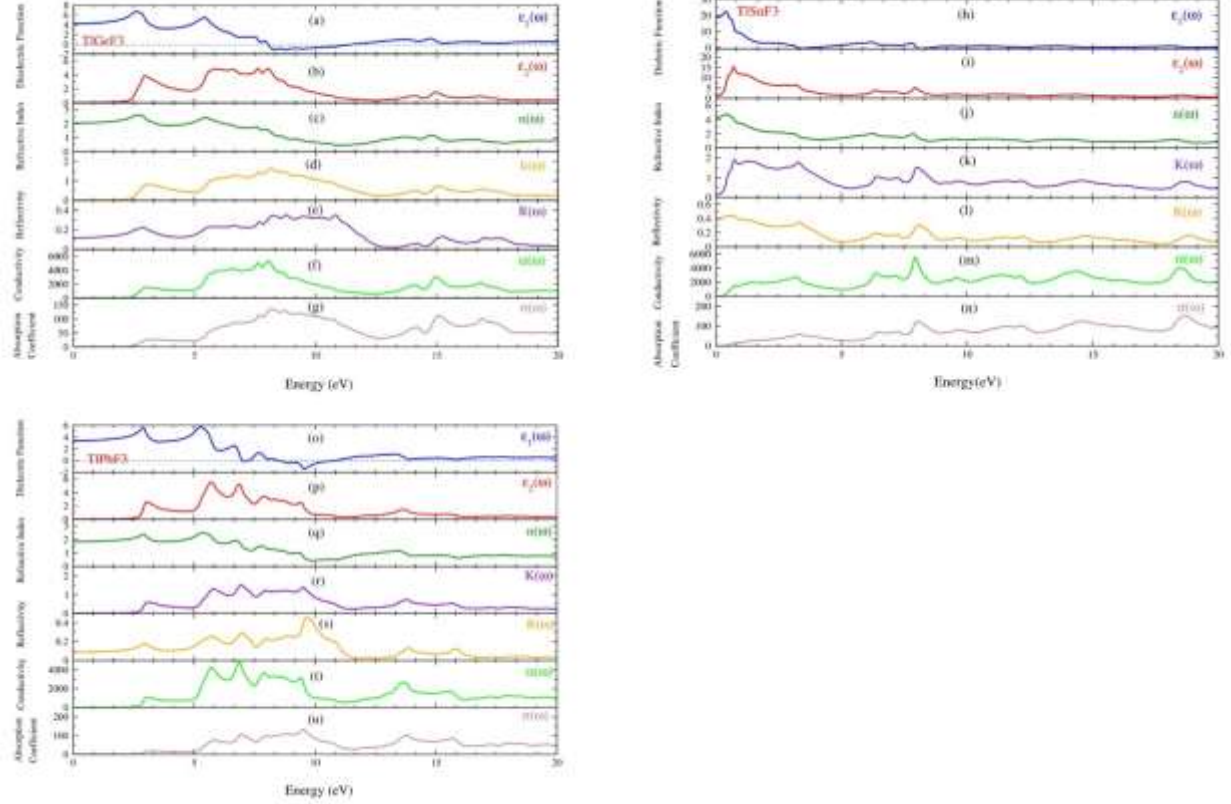


**Fig. 5.** Optical properties of  $\text{TlGeF}_3$ ,  $\text{TlSnF}_3$ , and  $\text{TlPbF}_3$  in the energy range of 0 to 20 eV.

The Refractive index is also an important complex parameter. Calculation of the refractive index and extinction coefficient has been done by using the following relations [21]

$$n(\omega) = \left[ \frac{\sqrt{\varepsilon_1^2(\omega) + \varepsilon_2^2(\omega)}}{2} + \frac{\varepsilon_1(\omega)}{2} \right]^{1/2} \quad (11)$$

$$k(\omega) = \left[ \frac{\sqrt{\varepsilon_1^2(\omega) + \varepsilon_2^2(\omega)}}{2} - \frac{\varepsilon_1(\omega)}{2} \right]^{1/2}. \quad (12)$$

Refractive index for  $\text{TlGeF}_3$ ,  $\text{TlSnF}_3$  and  $\text{TlPbF}_3$  has been displayed in Fig. 5(c), (j) and (q). The static refractive indices have values of 2.0, 4.3, and 1.8 for  $\text{TlGeF}_3$ ,  $\text{TlSnF}_3$ , and  $\text{TlPbF}_3$ . The refractive index of  $\text{TlGeF}_3$  and  $\text{TlPbF}_3$  is almost constant at lower photon energies. This represents optically isotropic behavior at lower energies. On the other hand, refractive index of  $\text{TlSnF}_3$  varies, exhibiting its optically anisotropic nature. While for high photon energies, the curve attains a maximum positive value. Beyond that, it displays a declining trend at higher photon energies. The extinction coefficients  $k(\omega)$  are presented in Fig. 5(d), (k), and (r). The maxima of extinction coefficient corresponding to the zero of  $\varepsilon_1(\omega)$  is 1.6 at 8.2 eV for  $\text{TlGeF}_3$ , 1.9 at 3.3 eV for  $\text{TlSnF}_3$ , and 1.5 at 6.9 eV for  $\text{TlPbF}_3$ .

The following relation can be used to calculate the Reflectivity of a solid.

$$R(\omega) = \left| \frac{(\varepsilon_1(\omega) + i\varepsilon_2(\omega))^{1/2} - 1}{(\varepsilon_1(\omega) + i\varepsilon_2(\omega))^{1/2} + 1} \right|. \quad (13)$$

Plots depicting the optical reflectivity are given in Fig. 5. (e), (l), and (s). The zero-frequency reflectivities for  $\text{TlGeF}_3$ ,  $\text{TlSnF}_3$  and  $\text{TlPbF}_3$  are 11%, 40% and 10% respectively. The reflectivity of a solid is either constant or has a smaller value for the energy range below the bandgap energy. The energy range in which the absorption capacity of a solid is maximum is the region in which the maximum reflectivity can be noted as shown by plots of  $\varepsilon_2(\omega)$ .

To determine optical conductivity and absorption coefficient following expressions are used

$$\sigma(\omega) = \frac{\omega}{4\pi} \varepsilon_2(\omega), \quad (14)$$

$$\alpha(\omega) = \sqrt{2}\omega \left[ \sqrt{\varepsilon_1^2(\omega) + \varepsilon_2^2(\omega)} - \varepsilon_1(\omega) \right]^{1/2}. \quad (15)$$

Optical conductivity of  $\text{TlAF}_3$  (A = Ge, Sn and Pb) are plotted in Fig. 5 (f), (m) and (t) while absorption coefficients are displayed in Fig. (g), (n), and (u) for all three compounds. Similar behavior is observed for both parameters in all energy range. Maximum absorption coefficient is observed about 142 at 8.2 eV for  $\text{TlGeF}_3$ , 153 at 18.7 eV for  $\text{TlSnF}_3$  and 140 at 9.6 eV for  $\text{TlPbF}_3$ . Above the bandgap energy, all the compounds show considerable absorption.

## 4. Conclusions

In this work, we investigated structural, elastic, and electronic properties as well as optical response to incident photons of Thallium-based heavy fluoropervoskites  $\text{TIAF}_3$  ( $A = \text{Ge}, \text{Pb}$  and  $\text{Sr}$ ) by using the GGA+U approach. The studied compounds are found to be structurally stable having values of optimized lattice constants in range (4.00-4.85 Å). The elastic parameters such as elastic constants, bulk modulus, anisotropy factor, Poisson's ratio, and Pugh's ratio are predicted. The Poisson ratio shows that understudy compounds are ductile. The ductile nature is also confirmed from the obtained values of the B/G ratio. The band structure and densities of states DOS for all compounds are analyzed. The band gaps of  $\text{TiGeF}_3$ ,  $\text{TiSnF}_3$  and  $\text{TiPbF}_3$  are calculated to be 1.67, 0.84, 1.89 eV, respectively. The optical properties such as dielectric function, refractive index, extinction coefficient, reflectivity, absorption coefficient, and optical conductivity are studied in the energy range of 0–20 eV. As the properties of these compounds are being reported for the first time, they could not be compared with other studies. Owing to cubic nature, structural stability and high effective atomic numbers, these compounds have potential to be used as X-ray and gamma-ray radiation detectors in single crystal form.

## Declarations

### Funding

Not Applicable

### Conflicts of interest/Competing interests

No conflicts of interest/competing interests

### Availability of data and material

Not Applicable

### Code availability

Not Applicable

## References

- [1] A. C. Garcia-Castro, N. A. Spaldin, A. H. Romero, and E. Bousquet, “Geometric ferroelectricity in fluoroperovskites,” *Phys. Rev. B - Condens. Matter Mater. Phys.*, vol. 89, no. 10, pp. 1–5, 2014.
- [2] T. Nishimatsu *et al.*, “Band structures of perovskite-like fluorides for vacuum-ultraviolet-transparent lens materials,” *Japanese J. Appl. Physics, Part 2 Lett.*, vol. 41, no. 4 A, pp. 10–13, 2002.

- [3] Y. L. Jing Hui Zeng, Ting Xie, Zhi Hua Li, “Monodispersed Nanocrystalline Fluoroperovskite Up-Conversion Phosphors,” *Cryst. Growth Des.*, vol. 7, pp. 2774–2777, 2007.
- [4] D. J. Daniel, O. Annalakshmi, U. Madhusoodanan, and P. Ramasamy, “Thermoluminescence characteristics and dosimetric aspects of fluoroperovskites ( $\text{NaMgF}_3:\text{Eu}^{2+},\text{Ce}^{3+}$ ),” *J. Rare Earths*, vol. 32, no. 6, pp. 496–500, 2014.
- [5] S. Körbel, M. A. L. Marques, and S. Botti, “Stability and electronic properties of new inorganic perovskites from high-throughput: Ab initio calculations,” *J. Mater. Chem. C*, vol. 4, no. 15, pp. 3157–3167, 2016.
- [6] S. Khan, S. U. Zaman, R. Ahmad, N. Mehmood, M. Arif, and H. J. Kim, “Ab initio investigations of structural, elastic, electronic and optical properties of the fluoroperovskite  $\text{TIXF}_3$  (X=Ca, Cd, Hg, and Mg) compounds,” *Mater. Res. Express*, vol. 6, p. 125923, 2019.
- [7] S. Khan *et al.*, “First-principles investigation of the physical properties of indium based fluoroperovskites  $\text{InAF}_3$  (A = Ca, Cd and Hg),” *Mater. Sci. Semicond. Process.*, vol. 121, no. August 2020, p. 105385, 2021.
- [8] M. J. Weber and R. . Monchamp, “Luminescence of  $\text{Bi}_4 \text{Ge}_3 \text{O}_{12}$  : Spectral and decay: Spectral and decay properties,” *J. Appl. Phys.*, vol. 44, no. 4, p. 5495, 1973.
- [9] K. Kamada *et al.*, “Composition engineering in cerium-doped  $(\text{Lu,Gd})_3(\text{Ga,Al})\text{5O}_{12}$  single-crystal scintillators,” *Cryst. Growth Des.*, vol. 11, no. 10, pp. 4484–4490, 2011.
- [10] H. J. Kim, G. Rooh, H. Park, and S. Kim, “Luminescence and scintillation properties of the new Ce-doped  $\text{Tl}_2\text{LiGdCl}_6$  single crystals,” *J. Lumin.*, vol. 164, pp. 86–89, 2015.
- [11] M. Kobayashi *et al.*, “Scintillation and phosphorescence of  $\text{PbWO}_4$  crystals,” *Nucl. Instruments Methods Phys. Res. Sect. A Accel. Spectrometers, Detect. Assoc. Equip.*, vol. 373, no. 3, pp. 333–346, 1996.
- [12] D. J. Singh, *Plane wave, Pseudopotential and LAWP Method*. Washington: Springer, 2006.
- [13] P. Blaha, K. Schwarz, F. Tran, R. Laskowski, G. K. H. Madsen, and L. D. Marks, “WIEN2k\_ An APW+lo program for calculating the properties of solids,” *J. Chem. Phys.*, vol. 152, p. 074101, 2020.
- [14] J. P. Perdew, K. Burke, and M. Ernzerhof, “Generalized gradient approximation made simple,” *Phys. Rev. Lett.*, vol. 77, no. 18, pp. 3865–3868, 1996.
- [15] F. D. Murnaghan, “The compressibility of media under extreme pressure,” *Proc. Natl. Acad. Sci. USA*, vol. 30, pp. 244–247, 1944.
- [16] G. Grimvall, *Thermophysical Properties of Materials*. Amsterdam: Elsevier, 1999.
- [17] R. Hill, “The elastic behaviour of a crystalline aggregate,” *Proc. Phys. Soc. Sect. A*, vol.

65, no. 5, pp. 349–354, 1952.

- [18] S. F. Pugh, “XCII. Relations between the elastic moduli and the plastic properties of polycrystalline pure metals,” *London, Edinburgh, Dublin Philos. Mag. J. Sci.*, vol. 45, no. 367, pp. 823–843, 1954.
- [19] S. A. B. I.N. Frantsevich, F.F. Voronov, *Elastic constants and elastic moduli of metals and insulators*. Kiev: Naukova, 1982.
- [20] C. Ambrosch-Draxl and J. O. Sofo, “Linear optical properties of solids within the full-potential linearized augmented planewave method,” *Comput. Phys. Commun.*, vol. 175, no. 1, pp. 1–14, 2006.
- [21] M. Dressel and G. Gruener, *Electrodynamics of Solids: Optical Properties of Electrons in Matter*. Cambridge University Press, UK, 2002.